ADVANCED MATERIALS
www.advmat.de

www.MaterialsViews.com

Highly Efficient, Simplified, Solution-Processed Thermally Activated Delayed-Fluorescence Organic Light-Emitting Diodes

*Young-Hoon Kim, Christoph Wolf, Himchan Cho, Su-Hun Jeong, and Tae-Woo Lee**

Thermally activated delayed-fluorescence (TADF) materials composed of low-cost pure organic complexes are promising for use in solid-state lighting sources and displays based on organic light-emitting diodes (OLEDs) due to the possibility of achieving 100% internal quantum efficiency (IQE) without using expensive metals such as Ir and Pt.[1,2] Generally, TADF materials have a very small energy gap between the lowest triplet excited state (T1) and the singlet excited state (S1), so they can turn 75% of excitons generated for phosphorescence to delayed fluorescence by reverse intersystem crossing.[1,2] Furthermore, TADF materials have advantages of easy synthesis using pure-organic molecules, versatile molecular design, and lower triplet and singlet energy levels than phosphorescence emitters, which can reduce the driving voltage in devices because host materials with narrower bandgap than bandgap of host materials in phosphorescence devices can be used.[1] Recently, researchers have achieved very high IQE of ≈94% using green-emitting pure-organic TADF materials, 2,4,5,6-tetra(carbazol-9-yl)-1,3-dicyanobenzene (4CzIPN), and external quantum efficiency (EQE) of ≈30% in 4CzIPN-based OLEDs; these efficiencies are comparable to those of phosphorescent materials and phosphorescence-based OLEDs.[1] However, these highly efficient TADF-OLEDs are fabricated using high-vacuum deposition, which entails a complex and expensive fabrication process, is difficult to apply to large areas, and is incompatible with roll-to-roll processes. Therefore, solution-processing methods that do not have these disadvantages should be evaluated.

Very recently, the potential of solution-processed TADF-OLEDs was demonstrated by synthesizing new pure-organic TADF materials; 2,4,5,6-tetra(3,6-di-tert-butylcarbazol-9-yl)-1,3-dicyanobenzene (t4CzIPN), which showed higher solubility (0.4%) in toluene than did 4CzIPN (0.1%), enabled fabrication of uniform emitting layer (EML) on a poly(3,4-ethylenedioxythiophene):poly(styrenesulfonate) (PEDOT:PSS)/poly(9-vinylcarbazole) (PVK) multilayer, and resulted in much improved device efficiencies (EQE ≈ 18.3% and power efficiency (PE) ≈ 42.7 lm W^{-1}) compared to 4CzIPN-based OLEDs (≈8.1% and ≈8.9 lm W^{-1}, respectively).[3] These EQE and PE values are higher than those of conventional solution-processed fluorescent OLEDs, but are still lower than those of vacuum deposited multilayer TADF-OLEDs. Furthermore, use of these PEDOT:PSS/PVK multilayer can make mass production of solution-processed TADF-OLEDs difficult due to the complex fabrication process.[4–6] Thus, the solution processed TADF devices should be further simplified without a hole transport layer (HTL) and the efficiency of the simplified devices should be boosted up to the level of vacuum-deposited multilayer TADF-OLEDs.

The efficiency of simplified TADF devices without HTL can be limited possibly due to the severe exciton quenching at the PEDOT:PSS/EML interface[7] and at the aggregation of TADF materials, which have long exciton lifetime (≥1 μs), in the EML due to poor solubility.[3,8] Therefore, we have to overcome luminescence quenching at the conducting hole injection layer (HIL)/EML interface and in the aggregated EML in simplified TADF-OLEDs.

Furthermore, making 4CzIPN with deep-lying highest occupied molecular orbital (HOMO) level feasible as a dopant in a solution-processed EML requires reduction of the large hole injection barrier from the indium tin oxide (ITO) anode to the EML. This barrier is caused by the deep HOMO level of host materials (≥5.9 eV), which must have deeper HOMO level than that of 4CzIPN (≈5.8 eV). One solution which reduces the hole injection barrier and luminescence quenching without HTL is to use a high-work-function (WF) HIL that can facilitate hole injection into a host material, which has a deeper HOMO level (≥5.9 eV) than does 4CzIPN (≈5.8 eV) in the EML, and that can prevent luminescence quenching at the HIL/EML interface. Conventional PEDOT:PSS has relatively low WF (≈5.2 eV) and causes a large hole injection barrier (≈0.7 eV) between the ITO anode and the EML.[5,7] This large hole injection barrier causes hole trapping at the HIL/EML interface as a consequence of inferior hole injection, induces the electron–hole imbalance in the EML, and reduces the overall efficiency of devices.[9] Furthermore, conducting PEDOT:PSS can induce severe luminescence quenching at the interface with TADF materials which have long exciton lifetime (≥1 μs).[1,7,8] Therefore, to achieve high EQE in solution-processed and simplified TADF-OLEDs without using a HTL on top of a HIL, the materials used as the HIL must be chosen carefully. After solving these issues, pure-organic TADF emitters can be strong candidates as low-cost dopants for solution-processed and simplified OLEDs.

To increase the hole injection capability and prevent luminescence quenching at the HIL/EML interface, we used a self-organized buffer HIL (Buf-HIL) that consists of PEDOT:PSS and a perfluorinated polymeric acid, tetrafluoroethylene-perfluoro-3,6-dioxa-4-methyl-7-octene-sulfonic acid copolymer (PFI) (**Figure 1**a).[5] We used 4,4′-bis(N-carbazolyl)-1,1′-biphenyl

Y.-H. Kim, C. Wolf, H. Cho, S.-H. Jeong, Prof. T.-W. Lee
Department of Materials Science and Engineering
Pohang University of Science and Technology (POSTECH)
Pohang, Gyungbuk 790-784, Republic of Korea
E-mail: twlee@postech.ac.kr; taewlees@gmail.com

DOI: 10.1002/adma.201504490

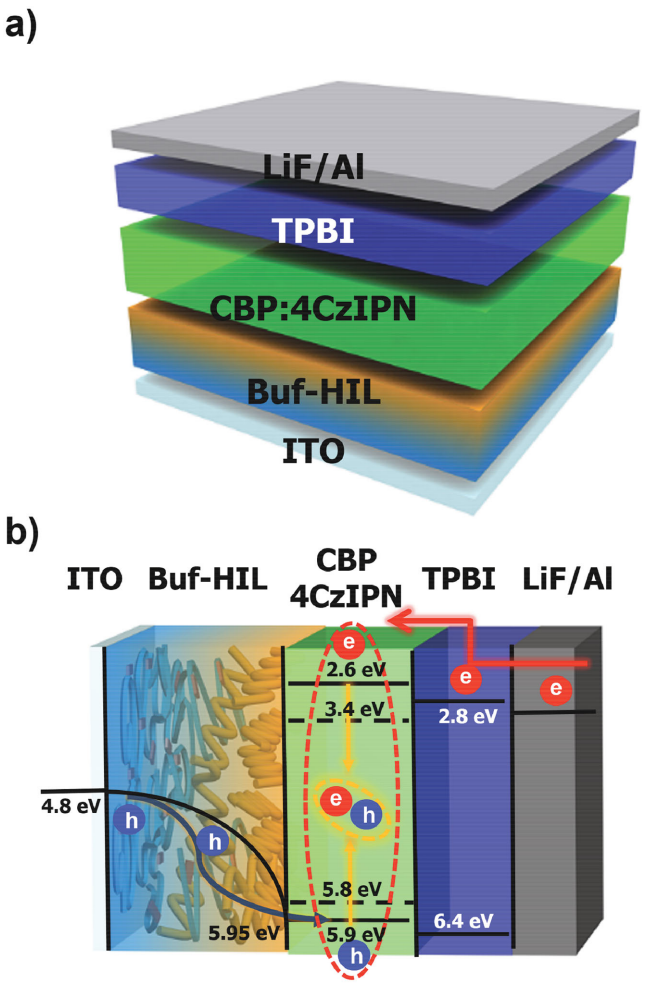

Figure 1. a) Solution-processed 4CzIPN-based OLED structure using Buf-HIL and b) energy level diagram of 4CzIPN-based OLEDs.

(CBP) as a host material in EML due to its deep HOMO level (≈5.9 eV), high triplet energy level (2.58 eV), and good bipolar charge mobility. PFI has lower surface energy than does PEDOT:PSS, so during spin-coating of the Buf-HIL, PFI rises to the top; this process leads to the formation of a self-organized Buf-HIL that has gradient PFI concentration [PFI] which increases gradually from the bottom to the top of the layer. PFI has deep ionization potential (IP), so this gradient [PFI] results in a gradual increase in the WF of Buf-HIL from ≈5.2 eV at the bottom surface to ≈5.95 eV at the top surface (Figure 1b and Table S1, Supporting Information).[5] This gradually increasing WF can facilitate hole injection to the HOMO of the CBP and can improve the hole–electron charge balance in the EML. The good match of the Buf-HIL WF with the CBP HOMO also decreases the hole accumulation at the HIL/EML interface and the internal field-induced exciton quenching at the interface, which in turn can increase the luminescent efficiency and reduce the overshoot of transient electroluminescence (Tr-EL).[9] This combination of improved hole injection capability from Buf-HIL to EML and decreased hole accumulation at the HIL/EML interface can be confirmed by capacitance-versus-voltage (*C*–*V*) measurement and Tr-EL measurement.

Furthermore, by increasing the distance between generated excitons and the conducting PEDOT:PSS,[7] the high [PFI] in the upper part of the Buf-HIL can reduce the severe luminescence quenching that occurs at the interface between semi-metallic PEDOT:PSS and 4CzIPN:CBP EML, which has long exciton lifetime (≥1 μs).[8] This blocking of exciton quenching can be confirmed by time-correlated single photon counting (TCSPC) measurement and steady-state photoluminescence (PL).

We also engineered the film of the EML to achieve a uniform distribution of dopants, which avoids exciton quenching induced by aggregation due to locally high concentration.[3] Specifically, a polar aprotic organic solvent must be used to improve the solubility of the high-PLQE 4CzIPN material due to its high dipole moment (≈3.95 D) and thereby to establish a uniform distribution of dopant in the EML and smooth spin-coated layer.[3,7,10] Here, we chose tetrahydrofuran (THF) as a solvent of the EML because 4CzIPN is much more soluble in THF (≥10 wt%) than in previously used toluene (≤1 wt%). This relatively high solubility of 4CzIPN in THF results in a much smoother surface than the surface obtained using 4CzIPN in toluene, and therefore can reduce both the leakage current and concentration quenching in the EML, and thereby improve the luminescent efficiency of OLED devices.

Thus, the proposed method provides the benefits of: i) facilitated hole injection into EML and reduced hole accumulation at the HIL/EML interface, ii) blocking of exciton quenching by Buf-HIL, and iii) reduced aggregation-induced exciton quenching and surface roughness by increasing the solubility of 4CzIPN in THF. This combination of benefits resulted in very high device EQE of ≈24% and current efficiency (CE) of ≈73 cd A^{-1}, which are much higher than those of PEDOT:PSS-based OLEDs (EQE ≈ 15% and CE ≈ 45 cd A^{-1}). To our best knowledge, these efficiencies are the best in solution-processed OLEDs based on pure-organic TADF materials. We also demonstrated high-efficiency red-emitting and blue-emitting solution-processed TADF-based OLEDs with simplified structure for the first time.

A CBP layer (≈40 nm) and CBP:4CzIPN layer (≈40 nm) were fabricated by spin-coating the solution dissolved in THF. The CBP layer had root-mean-square roughness r_{rms} of ≈0.285 nm and the CBP:4CzIPN layer had r_{rms} of ≈0.278 nm (**Figure 2**a,b). These similar rms values between CBP layer with and without 4CzIPN are due to the high solubility of 4CzIPN in THF. However, although a CBP layer fabricated from toluene solution showed low r_{rms} of ≈0.473, a CBP:4CzIPN layer fabricated from toluene solution showed much higher r_{rms} of ≈2.04 and many peaks >20 nm; these characteristics resulted from aggregation of 4CzIPN due to its low solubility in toluene (Figure S1, Supporting Information) and lead to aggregation-induced exciton quenching; these results correspond well with previous research.[3] This high roughness can induce leakage current and reduce the efficiency in devices. The aggregated and non-uniformly dispersed dopant molecules in the host matrix can also induce exciton quenching in the layer, and consequently reduce the luminescent efficiency of solution-processed TADF-OLEDs.[3] These comparisons demonstrate that THF does not induce aggregation of 4CzIPN, and can increase the efficiency of solution-processed OLED by enabling formation of a uniform film.

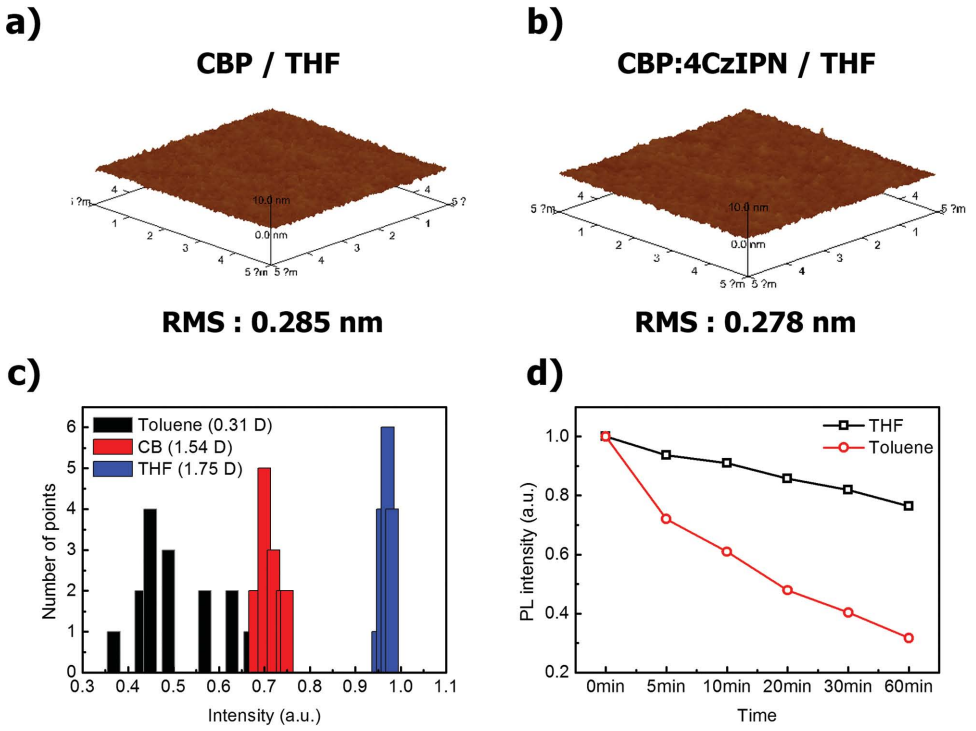

Figure 2. Atomic force microscopy (AFM) images of solution-processed a) CBP layer and b) CBP:4CzIPN layer dissolved in THF, c) histogram of maximum PL intensity measured for 15 points in CBP:4CzIPN layer dissolved in toluene, CB, and THF, and d) PL intensity change of CBP:4CzIPN layer dissolved in toluene and THF under λ = 350 nm excitation from a Xe lamp.

The aggregation or uniformity of dopant molecules in the CBP:4CzIPN layer was quantified by measuring the steady-state PL on different spots of CBP:4CzIPN films (≈40 nm), which were spin-cast from various solutions dissolved in toluene, chlorobenzene (CB), and THF on glass (Figure 2c). As the dipole moment of solvents increased from 0.31 D (toluene) to 1.75 D (THF), average PL intensity of films cast from the THF solution was doubled compared with that from the toluene solution, and the standard deviation of PL intensity of films cast from the THF solution is 0.98% which is much smaller than that from the toluene solution (9.52%) (Figure 2c and Figure S2, Supporting Information). This result implies that as the dipole moment of the solvent increases, dissolution of 4CzIPN dopants with high dipole moment (≈3.95 D) was improved in the CBP matrix, reduced the aggregation of 4CzIPN, and increased the PL intensity of the resulting uniform CBP:4CzIPN layer.[11,12] The aggregated and non-uniformly dispersed dopants in the CBP:4CzIPN layer cast from toluene solution also showed much faster PL decay under wavelength λ = 350 nm illumination from a Xe lamp than did the CBP:4CzIPN layer in the THF solution (Figure 2d and Figure S3, Supporting Information). Solution processing with THF, which provides much improved solubility of 4CzIPN, not only improved the layer uniformity and the PL intensity but also improved the photostability of the EML by minimizing the aggregation and maximizing the dopant uniformity in the host matrix.[11,12]

The Buf-HIL with a high WF (5.95 eV) can increase the efficiency of hole injection into the HOMO of CBP (≈5.9 eV) compared with PEDOT:PSS that has a low WF (≈5.2 eV). The gradually increased WF in the Buf-HIL can facilitate the hole injection to the HOMO of CBP and improve the hole–electron charge balance in EML. To verify the effect of [PFI] on hole injection capability, we conducted *C–V* measurements using solution-processed TADF-OLEDs with different HILs (Glass/PEDOT:PSS or Buf-HIL (≈40 nm)/CBP:4CzIPN (≈40 nm)/1,3,5-*tris*(1-phenyl-1H-benzimidazol-2-yl)benzene (TPBI) (50 nm)/LiF (1 nm)/Al (100 nm)) (**Figure 3**a). As the majority carriers were injected to the organic layer, capacitance peak increased sharply; then after minority carriers were injected and recombined with majority carriers, the capacitance peak decreased quickly.[13,14] Thus, peak capacitance C_{peak} and the voltage at C_{peak} are related to the charge injection, transport, and accumulation behavior in these devices. PEDOT:PSS-based OLEDs showed delayed maximum peak voltage (≈8.7 V) compared with Buf-HIL-based OLEDs (≈6.8 V, respectively); this difference means that the Buf-HIL has much higher hole injection capability than does PEDOT:PSS, so use of the Buf-HIL results in low turn-on voltage and better electron–hole balance in the EML than does use of the PEDOT:PSS HIL. Buf-HIL-based OLEDs also showed lower C_{peak} than did PEDOT:PSS-based OLEDs, because in the latter, the large hole injection barrier (≈0.7 eV) between PEDOT:PSS and the EML results in large accumulation of holes at the interface and high C_{peak}.[13,14]

The reduced hole accumulation at the Buf-HIL/EML interface can be verified by Tr-EL measurements (Figure 3b). In the PEDOT:PSS-based OLEDs, holes accumulate at the PEDOT:PSS/EML interface under bias due to the large hole injection barrier; this accumulation generates an internal electric field at the HIL/EML interface, then induces

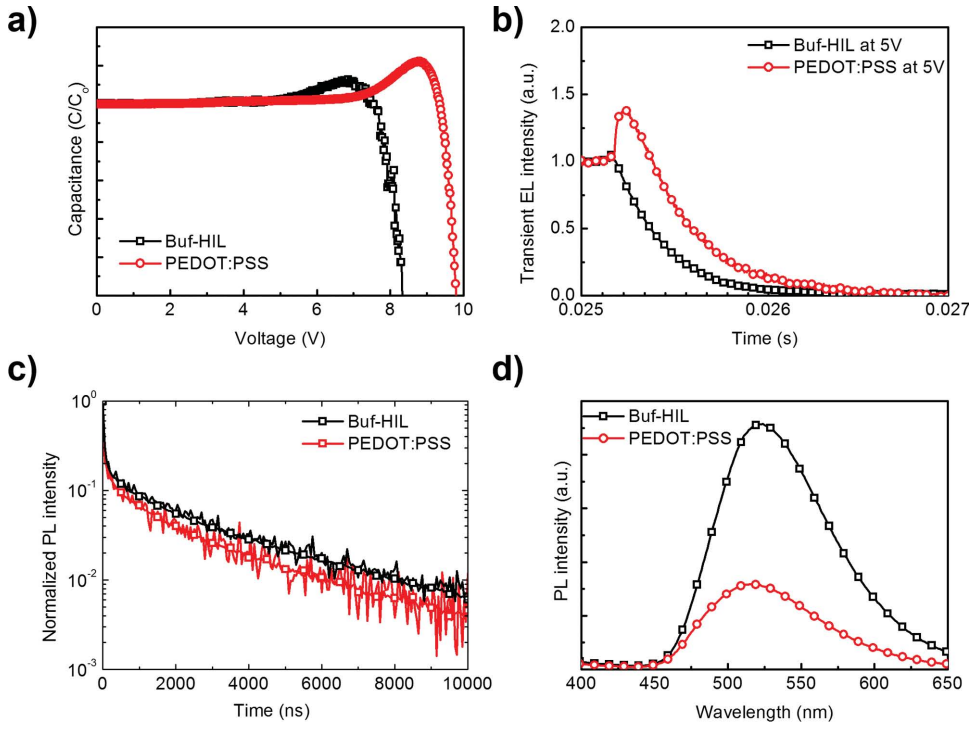

Figure 3. a) Capacitance-versus-voltage characteristics, b) transient electroluminescence characteristics of solution-processed 4CzIPN-based OLEDs using Buf-HIL and PEDOT:PSS at 5 V, c) PL lifetime curves obtained from TCSPC, and d) PL intensities of thin solution-processed CBP:4CzIPN layer on Buf-HIL and PEDOT:PSS.

exciton–polaron annihilation and low luminescent efficiency.[9] The accumulated holes at the PEDOT:PSS/EML interface cause a local electric field, which also induce quenching of excitons adjacent to the interface when bias is applied; this quenching reduced the device efficiency under electric field. When the bias is turned off, most of the accumulated holes immediately dissipate by diffusing to the ITO anode. This sudden dissipation of accumulated hole charges reduces the local electric field and the exciton quenching adjacent to the interface, and thereby induces a large transient overshoot in the transient turn-off region. Thus, PEDOT:PSS-based OLEDs showed larger transient overshoot than did Buf-HIL-based OLEDs. As the bias increased, the increasing external field reduced the hole accumulation at the PEDOT:PSS/EML interface, so transient overshoot intensity caused by this hole accumulation decreased gradually (Figure S4, Supporting Information). However, Buf-HIL-based OLEDs showed almost no transient overshoot at every bias; this observation means that at every bias, the Buf-HIL facilitates hole injection into the EML without trapping at the interface. Therefore, the gradually increasing WF from bottom to top in the HIL can improve luminescent efficiency both by facilitating hole injection into the EML, and by reducing the charge accumulation at the HIL/EML interface.

The large [PFI] at the top of Buf-HIL can reduce the luminescence quenching that occurs at the PEDOT:PSS/EML interface.[7] To verify the luminescence quenching blocking effect of PFI, we conducted TCSPC with thin solution-processed CBP:4CzIPN layer on different under-layers (glass/PEDOT:PSS or Buf-HIL (≈40 nm)/CBP:4CzIPN (≈10 nm)) (Figure 3c). The data were fitted using a bi-exponential function that represents two PL decay pathways: i) initial fluorescence of 4CzIPN, and ii) TADF due to the reverse intersystem crossing.[15] Buf-HIL/CBP:4CzIPN showed longer average PL lifetime (2.223 μs) than did PEDOT:PSS/CBP:4CzIPN (1.693 μs). This result means that the large [PFI] in the Buf-HIL provides a buffer between the PEDOT:PSS surface and the excitons that originated in the EML, then reduces the luminescence quenching caused by: i) exciton dissociation facilitated by the energy level difference between HOMO level of EML (≈5.9 eV) and WF of under-layers (≈5.2 eV for PEDOT:PSS; ≈5.9 eV for Buf-HIL), and ii) nonradiative energy transfer from the EML to the PEDOT:PSS.[5,7] This Buf-HIL that blocks the exciton quenching at the HIL/EML interface may be essential to realize high-efficiency simple-structured OLEDs, especially using TADF emitters that have long exciton lifetime.

The Buf-HIL's blocking of exciton quenching can be quantified by measuring steady-state PL with a thin solution-processed CBP:4CzIPN layer on different under-layers (glass/PEDOT:PSS or Buf-HIL (≈40 nm)/CBP:4CzIPN (≈10 nm)) (Figure 3d). Samples were excited with monochromated light-source (λ = 320 nm). Buf-HIL/CBP:4CzIPN showed much higher PL peak intensity than did the PEDOT:PSS/CBP:4CzIPN. The difference occurs because the thick PFI layer on the top surface of the Buf-HIL reduced the exciton quenching by keeping the excitons away from the PEDOT:PSS. Therefore, the Buf-HIL increases the luminescent efficiency in the simplified TADF-OLED devices by: i) facilitating hole injection and reducing the accumulation of holes at the HIL/EML interface, and ii) blocking the exciton quenching even in a simplified structure.

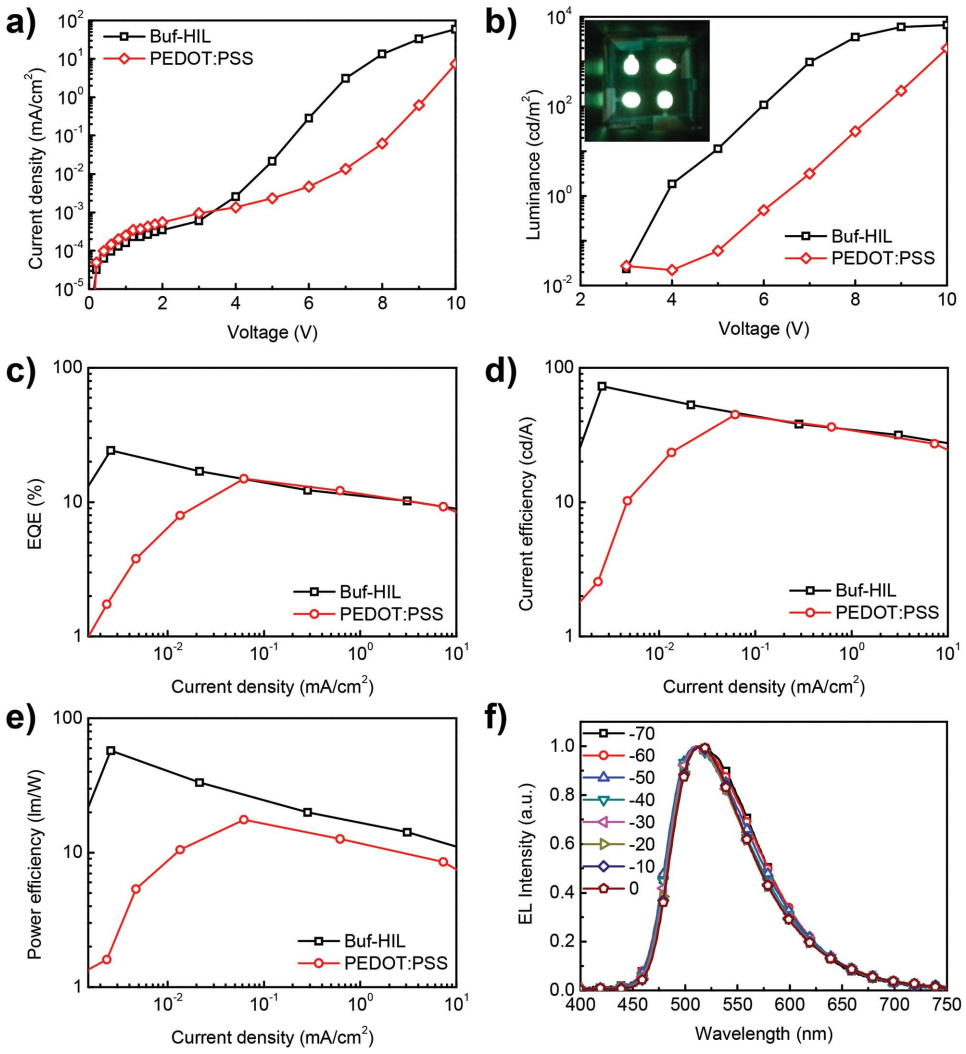

Figure 4. a) Current density versus voltage characteristics, b) luminance versus voltage characteristics and optical image of green light emission from devices using Buf-HIL (inset), c) external quantum efficiency versus current density characteristics, d) current efficiency versus current density characteristics, e) power efficiency versus current density characteristics of solution-processed 4CzIPN-based OLEDs using Buf-HIL and PEDOT:PSS, and f) electroluminescence spectrum of solution-processed OLEDs at the different viewing angle.

TADF-OLEDs that used a Buf-HIL (Glass/ITO/Buf-HIL/CBP:4CzIPN/TPBI/LiF/Al) showed higher current density under operating voltages >3.5 V than did devices that used PEDOT:PSS (**Figure 4**a). The increase in current density demonstrates that the gradually increasing WF of Buf-HIL can reduce the hole injection barrier from the ITO anode to the HOMO of CBP, and thereby facilitate hole injection into the EML.[16] Buf-HIL-based OLEDs also showed much lower turn-on voltage (3.8 V at 1 cd m^{-2}) and operating voltage (7 V at 1000 cd m^{-2}) than did PEDOT:PSS-based OLEDs (6.4 and 9.7 V, respectively) (Figure 4b). Buf-HIL-based OLEDs showed very bright green emission (inset). Buf-HIL-based OLEDs attained EQE of ≈24%, CE of ≈73 cd A^{-1}, and PE of ≈58 lm W^{-1}, which are much greater than those of PEDOT:PSS-based OLEDs (EQE ≈ 15%, CE ≈ 43 cd A^{-1}, PE ≈ 17.56 lm W^{-1}); to the best of our knowledge, these are the highest luminescence efficiencies in solution-processed OLEDs based on pure-organic TADF emitters to date (Figure 4c–e). These improved EQE, CE, and PE emphasize the superior hole injection capability and exciton quenching blocking capability of PFI in Buf-HIL, which are important factors to increase the luminescent efficiency in our simplified TADF-OLEDs that use emitters which have very long exciton lifetime (≥1 µs). The PL spectra of the Buf-HIL-based solution-processed TADF-OLEDs were not affected by viewing angle; this is an important attribute for application of displays and solid-state lighting (Figure 4f).

We also fabricated the first solution-processed TADF red-emitting OLEDs that use 1,4-dicyano-2,3,5,6-tetrakis(3,6-diphenylcarbazol-9-yl)benzene (4CzTPN-Ph) as a red-emitting dopant using the same simplified device structure (**Figure 5**a,b, inset). These red-emitting TADF-OLEDs had EQE of ≈13.3%, CE of ≈30 cd A^{-1}, and PE of ≈23.5 lm W^{-1}, which are much higher than those of conventional fluorescence red-emitting OLEDs (Figure 5a,b and Figure S5a, Supporting Information).[17,18] The PL spectra of these red-emitting OLEDs also did not change with viewing angle (Figure S5b, Supporting Information).

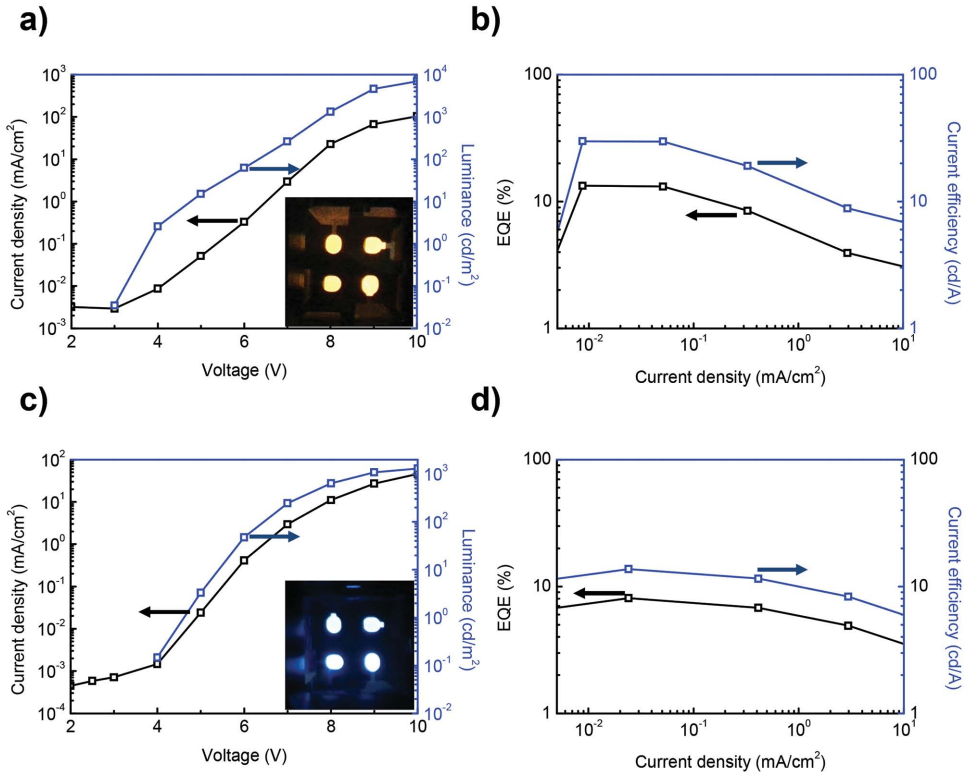

Figure 5. a) Current density versus voltage, luminance versus voltage characteristics and optical image of red light emission from devices using Buf-HIL (inset), b) External quantum efficiency versus current density and current efficiency versus current density characteristics of solution-processed red-emitting 4CzTPN-Ph-based OLEDs using Buf-HIL, c) Current density versus voltage, luminance versus voltage characteristics and optical image of blue light emission from devices using Buf-HIL (inset), and d) External quantum efficiency versus current density and current efficiency versus current density characteristics of solution-processed blue-emitting 2CzPN-based OLEDs using Buf-HIL.

Finally, we fabricated solution-processed TADF blue-emitting OLEDs using 1,2-bis(carbazol-9-yl)-4,5-dicyanobenzene (2CzPN) as a blue-emitting dopant and 1,3-bis(9H-carbazol-9-yl)-benzene (mCP) as a host (Figure 5c,d, inset);[19] to the best of our knowledge, this is the first such device. These blue-emitting solution-processed OLEDs showed higher device efficiencies (EQE ≈ 8.1%, CE ≈ 14 cd A^{-1}, PE ≈ 8.6 lm W^{-1}) than conventional fluorescence blue-emitting OLEDs (Figure 5c,d and Figure S5c, Supporting Information).[18,20]

In conclusion, we have demonstrated highly efficient, solution-processed green-emitting TADF-OLEDs with a simplified structure by efficiently managing the exciton quenching which occurs at HIL/EML interface and in the aggregated EML, and by facilitating hole injection from the anode and reducing the hole accumulation at HIL/EML interface. We used a multifunctional Buf-HIL that has a high WF and a surface-enriched PFI layer on the top of Buf-HIL. The Buf-HIL with significantly increased WF improved hole injection capability by reducing the hole injection barrier into the EML. The Buf-HIL also reduced the hole accumulation at the HIL/EML interface, reduced the local-electric-field-induced exciton quenching, and improved the hole–electron balance in the EML. Furthermore, Buf-HIL improved the luminescent efficiency by blocking exciton quenching which occurs at the HIL/EML interface. To avoid aggregation-induced exciton quenching in the EML, we used polar aprotic organic solvent to achieve uniform distribution of 4CzIPN dopants in the CBP host and uniform thickness of the EML film because this solvent provides good solubility of polar-emitting dopants. As a result, very good solubility of the TADF dopant in the EML by high-solubility-solvent and important synergetic role of the Buf-HIL can improve the radiative recombination in the EML and device efficiency even in a simplified structure. Our simplified OLEDs fabricated using these methods achieved EQE of ≈24%, CE of ≈73 cd A^{-1}, and PE of ≈58 lm W^{-1}, which are much higher than those of TADF-OLEDs that use conventional PEDOT:PSS (EQE ≈ 15%, CE ≈ 43 cd A^{-1}, PE ≈ 17.56 lm W^{-1}). To the best of our best knowledge, these are the highest efficiencies in solution-processed OLEDs based on pure-organic TADF emitters to date. We also demonstrated first high-efficiency red-emitting and blue-emitting solution-processed TADF-OLEDs that use simple structure and pure-organic emitters.

Our work suggests a new method to produce high-efficiency solution-processed OLEDs which should solve two challenges at the same time: i) reducing the price of the dopant by eliminating the need for costly materials such as Ir and Pt; and ii) simplifying the structure while maintaining high luminescent efficiency by reducing the exciton quenching and improving electron–hole balance. High-efficiency solution-processed, simplified OLEDs can be achieved using this strategy that uses: i) well-dispersed pure-organic dopant, TADF emitters, which can achieve IQE close to 100%, and manage the

exciton quenching in the EML by reducing the aggregation, and ii) Buf-HIL to increase the hole-injection capability and to block the exciton quenching at the HIL/EML interface. Although scientific and technological roadmaps have anticipated that future flexible OLEDs would be commercialized as solution-processed polymer light-emitting diodes (PLEDs) due to simple structure,[21] our high-efficiency simplified OLED strategy using pure-organic TADF emitters and multifunctional Buf-HIL can realize large-area displays and solid-state lighting based on solution-processed small-molecule-based devices.

Experimental Section

Device Fabrication: Patterned ITO-coated glasses were sonicated in acetone and in 2-propanol for 15 min sequentially, then treated with UV-ozone for 10 min to make the surface hydrophilic. Then PEDOT:PSS or Buf-HIL were spin-coated in the ambient condition to give a 40-nm-thick HIL and baked at 150 °C for 30 min. EML solution containing CBP and TADF dopant was spin-coated to give 40-nm thickness, then baked in an N_2-filled glove box to remove the residual solvent. Then TPBI (50 nm), LiF (1 nm), and Al (100 nm) were deposited sequentially in a high vacuum chamber ($<10^{-7}$ Torr).

OLED Characterization: The current–voltage–luminance characteristics were measured using a Keithley 236 source measurement unit and Minolta CS2000 spectroradiometer.

PL Measurement: PL data were measured using a JASCO FP6500 spectrofluorometer.

TCSPC Measurement: A pulsed ND:YAG laser with λ = 355 nm was used as the excitation source, and an intensified charge-coupled device was used as a detector.

Supporting Information

Supporting Information is available from the Wiley Online Library or from the author.

Acknowledgements

This work was supported by the National Research Foundation of Korea (NRF) grant funded by the Korea government (MSIP) (Grant No. NRF-2013R1A2A2A01068753). This work was also supported by the Center for Advanced Soft-Electronics funded by the Ministry of Science, ICT, and Future Planning as Global Frontier Project (Grant No. 2014M3A6A5060947).

Received: September 13, 2015
Revised: October 15, 2015
Published online: November 30, 2015

[1] a) H. Uoyama, K. Goushi, K. Shizu, H. Nomura, C. Adachi, *Nature* **2012**, *492*, 234; b) B. S. Kim, J. Y. Lee, *Adv. Funct. Mater.* **2014**, *24*, 3970; c) Y. J. Cho, K. S. Yook, J. Y. Lee, *Adv. Mater.* **2014**, *26*, 4050; d) J. W. Sun, J.-H. Lee, C.-K. Moon, K.-H. Kim, H. Shin, J.-J. Kim, *Adv. Mater.* **2014**, *26*, 5684; e) M. P. Gaj, C. F. Hernandez, Y. Zhang, S. R. Marder, B. Kippelen, *Org. Electron.* **2015**, *16*, 109; f) H. Nakanotani, K. Masui, J. Nishide, T. Shibata, C. Adachi, *Sci. Rep.* **2013**, *3*, 2127.

[2] a) C.-J. Chiang, A. Kimyonok, M. K. Etherington, G. C. Griffiths, V. Jankus, F. Turksoy, A. P. Monkman, *Adv. Funct. Mater.* **2013**, *23*, 739; b) W. Li, Y. Pan, R. Xiao, Q. Peng, S. Zhang, D. Ma, F. Li, F. Shen, Y. Wang, B. Yang, Y. Ma, *Adv. Funct. Mater.* **2014**, *24*, 1609; c) D. Graves, V. Jankus, F. B. Dias, A. Monkman, *Adv. Funct. Mater.* **2014**, *24*, 2343; d) C. Mayr, S. Y. Lee, T. D. Schmidt, T. Yasuda, C. Adachi, W. Brütting, *Adv. Funct. Mater.* **2014**, *24*, 5232; e) F. B. Dias, K. N. Bourdakos, V. Jankus, K. C. Moss, K. T. Kamtekar, V. Bhalla, J. Santos, M. R. Bryce, A. P. Monkman, *Adv. Mater.* **2013**, *25*, 3707; f) G. Méhes, H. Nomura, Q. Zhang, T. Nakagawa, C. Adachi, *Angew. Chem. Int. Ed.* **2012**, *51*, 11311; g) D. Zhang, L. Duan, Y. Li, D. Zhang, Y. Qiu, *J. Mater. Chem. C* **2014**, *2*, 8191.

[3] Y. J. Cho, K. S. Yook, J. Y. Lee, *Adv. Mater.* **2014**, *26*, 6642.

[4] a) B. W. D'Andrade, S. R. Forrest, *Adv. Mater.* **2004**, *16*, 1585; b) Y. Sun, N. C. Giebink, H. Kanno, B. Ma, M. E. Thompson, S. R. Forrest, *Nature* **2006**, *440*, 908; c) X. Zhou, J. Blochwitz, M. Pfeiffer, A. Nollau, T. Fritz, K. Leo, *Adv. Funct. Mater.* **2001**, *11*, 310; d) H.-W. Lin, W.-C. Lin, J.-H. Chang, C.-I. Wu, *Org. Electron.* **2013**, *14*, 1204.

[5] a) T.-W. Lee, Y. Chung, O. Kwon, J.-J. Park, *Adv. Funct. Mater.* **2007**, *17*, 390; b) Y.-H. Kim, H. Cho, J. H. Heo, T.-S. Kim, N. Myung, C.-L. Lee, S. H. Im, T.-W. Lee, *Adv. Mater.* **2015**, *27*, 1248.

[6] a) R. Komatsu, H. Sasabe, S. Inomata, Y.-J. Pu, J. Kido, *Synth. Met.* **2015**, *202*, 165; b) A. Perumal, H. Faber, N. Yaacobi-Gross, P. Pattanasattayavong, C. Burgess, S. Jha, M. A. McLachlan, P. N. Stavrinou, T. D. Anthopoulos, D. D. C. Bradley, *Adv. Mater.* **2015**, *27*, 93; c) T. Chiba, Y.-J. Pu, J. Kido, *Adv. Mater.* **2015**, *27*, 4681.

[7] a) Y. Suzuki, Q. Zhang, C. Adachi, *J. Mater. Chem. C* **2015**, *3*, 1700; b) T.-H. Han, M.-R. Choi, S.-H. Woo, S.-Y. Min, C.-L. Lee, T.-W. Lee, *Adv. Mater.* **2012**, *24*, 1487; c) J.-S. Kim, R. H. Friend, I. Grizzi, J. H. Burroughes, *Appl. Phys. Lett.* **2005**, *87*, 023506; d) A. V. Dijken, A. Perro, E. A. Meulenkamp, K. Brunner, *Org. Electron.* **2003**, *4*, 131; e) H. Yan, B. J. Scott, Q. Huang, T. J. Marks, *Adv. Mater.* **2004**, *16*, 1948; f) T.-W. Lee, M.-G. Kim, S. Y. Kim, S. H. Park, O. Kwon, T. Noh, T.-S. Oh, *Appl. Phys. Lett.* **2006**, *89*, 123505.

[8] A. S. D. Sandanayaka, K. Yoshida, T. Matsushima, C. Adachi, *J. Phys. Chem. C* **2015**, *119*, 7631.

[9] a) R. Liu, Z. Gan, R. Shinar, J. Shinar, *Phys. Rev. B* **2011**, *83*, 245302; b) S. Lee, K.-H. Kim, D. Limbach, Y.-S. Park, J.-J. Kim, *Adv. Funct. Mater.* **2013**, *23*, 4105; c) D. Zhang, L. Duan, C. Li, Y. Li, H. Li, D. Zhang, Y. Qiu, *Adv. Mater.* **2014**, *26*, 5050.

[10] Y. Noguchi, H.-J. Kim, R. Ishino, K. Goushi, C. Adachi, Y. Nakayama, H. Ishii, *Org. Electron.* **2015**, *17*, 184.

[11] J.-R. Gong, L.-J. Wan, S.-B. Lei, C.-L. Bai, X.-H. Zhang, S.-T. Lee, *J. Phys. Chem. B* **2005**, *109*, 1675.

[12] Z. Xu, G. Y. Zhong, X. M. Ding, E. Obbard, H. J. Ding, X. J. Wang, Y. Q. Zhan, S. T. Zhang, J. M. Zhao, B. L. Zhao, Z. H. Xiong, H. Z. Shi, W. Huang, X. Y. Hou, *Appl. Phys. A* **2005**, *80*, 1753.

[13] T.-H. Han, W. Song, T.-W. Lee, *ACS Appl. Mater. Interfaces* **2015**, *7*, 3117.

[14] V. Shrotriya, Y. Yang, *J. Appl. Phys.* **2005**, *97*, 054504.

[15] a) T. Nishimoto, T. Yasuda, S. Y. Lee, R. Kondo, C. Adachi, *Mater. Horiz.* **2014**, *1*, 264; b) M. Kim, S. K. Jeon, S.-H. Hwang, J. Y. Lee, *Adv. Mater.* **2015**, *27*, 2515.

[16] T.-W. Lee, Y. Chung, *Adv. Funct. Mater.* **2008**, *18*, 2246.

[17] C.-T. Chen, *Chem. Mater.* **2004**, *16*, 4389.

[18] a) M. C. Gather, A. Köhnen, A. Falcou, H. Becker, K. Meerholz, *Adv. Funct. Mater.* **2007**, *17*, 191; b) J.-H. Jou, Y.-S. Chiu, C.-P. Wang, R.-Y. Wang, H.-C. Hu, *Appl. Phys. Lett.* **2006**, *88*, 193501; c) Y.-J. Pu, M. Higashidate, K.-I. Nakayama, J. Kido, *J. Mater. Chem.* **2008**, *18*, 4183; d) C. D. Müller, A. Falcou, N. Reckefuss, M. Rojahn, V. Wiederhirn, P. Rudati, H. Frohne, O. Nuyken, H. Becker, K. Meerholz, *Nature* **2003**, *421*, 829.

[19] D. Zhang, L. Duan, Y. Li, D. Zhang, Y. Qiu, *J. Mater. Chem. C* **2014**, *2*, 8191.
[20] a) C. Liu, Y. Li, Y. Zhang, C. Yang, H. Wu, J. Qin, Y. Cao, *Chem. Eur. J.* **2012**, *18*, 6928; b) Y. Li, Z. Wang, X. Li, G. Xie, D. Chen, Y.-F. Wang, C.-C. Lo, A. Lien, J. Peng, Y. Cao, S.-J. Su, *Chem. Mater.* **2015**, *27*, 1100; c) X. Zhan, N. Sun, Z. Wu, J. Tu, L. Yuan, X. Tang, Y. Xie, Q. Peng, Y. Dong, Q. Li, D. Ma, Z. Li, *Chem. Mater.* **2015**, *27*, 1847; d) D. Liu, M. Du, D. Chen, K. Ye, Z. Zhang, Y. Liu, Y. Wang, *J. Mater. Chem. C* **2015**, *3*, 4394; e) C. Yao, Y. Yu, X. Yang, H. Zhang, Z. Huang, X. Xu, G. Zhou, L. Yue, Z. Wu, *J. Mater. Chem. C* **2015**, *3*, 5783; f) S. Lee, B. R. Lee, J.-S. Kim, M. H. Song, *J. Mater. C* **2014**, *2*, 8673; g) R. Trattnig, L. Pevzner, M. Jäger, R. Schlesinger, M. V. Nardi, G. Ligorio, C. Christodoulou, N. Koch, M. Baumgarten, K. Müllen, E. J. W. List, *Adv. Funct. Mater.* **2013**, *23*, 4897; h) H. Park, J. Lee, I. Kang, H. Y. Chu, J.-I. Lee, S.-K. Kwon, Y.-H. Kim, J. Mater. *Chem.* **2012**, *22*, 2695; i) L.-P. Lu, D. Kabra, K. Johnson, R. H. Friend, *Adv. Funct. Mater.* **2012**, *22*, 144.
[21] Y.-H. Kim, T.-H. Han, H. Cho, S.-Y. Min, C.-L. Lee, T.-W. Lee, *Adv. Funct. Mater.* **2014**, *24*, 3808.